

Experimental heat transfer due to impinging of water from multiple jets on a heated surface

Mohamed Teamah^a and Sameh Farahat^b

^a Mechanical Eng. Dept., Faculty of Eng., Alexandria University, Alexandria, Egypt

^b Marine Eng. Technology Dept., College of MT and T, AASTMT, Alexandria, Egypt

Heat transfer due to the impingement of vertical circular jets on a horizontal heated surface is investigated experimentally. The water flow rates of 1, 5 and 8 liter/min per jet were used. Comparisons between single and multiple jets in different situation were carried out. The comparisons show that, in case of multi jets an interaction appeared between the jets. The effect of interaction between jets in multi jets tends to reduce both segment and average segment Nusselt numbers for any jet of multi jets compared with condition of single jet through the jump area. But the overall average Nusselt number on the plate area for multi jets for any arrangement was higher than that for single jet with the same flow rate. To reduce the effect of interaction between the jets, it is required to increase nozzle-to-nozzle separating distance. هذا البحث يتناول دراسة انتقال الحرارة و السريان نتيجة تصادم نافورات متعددة بسطح أفقي ساخن و لتحقيق هذا الهدف تمت الدراسة باستخدام التجارب المعملية فتم تصميم جهاز لعمل التجارب المعملية. أجريت التجارب للنافورات المتعددة لأربع توزيعات هندسية هم نافورتين متجاورتين و ثلاث نافورات موزعة على شكل خط مستقيم على مسافات متساوية و ثلاث نافورات موزعة على شكل زاوية قائمة مع تساوى الخطوتين الطولية و العمودية بين مراكز النافورات و تسعة نافورات موزعة على شكل مربعات. تمت هذه الدراسة المعملية لثلاث قيم لمعدل السريان هم 1 و 5 و 8 لتر/دقيقة. و بعد قياس درجات الحرارة الموضعية لكل من الماء و اللوح أمكن حساب كل من معامل انتقال الحرارة الموضعي و المتوسط عند مسافات متعددة من مركز النافورة و ذلك بعد عمل اتزان حراري بمساواة الطاقة الحرارية المكتسبة للماء بالطاقة الحرارية المنقلة بالحمل من اللوح للماء. أمكن استنتاج بعض النقاط الهامة و هي أنه نتيجة التداخل بين النافورات نقل سرعة الماء و تزيد سمك طبقة الماء و ينخفض معامل انتقال الحرارة في منطقة التداخل فقط. ولكن قيمته للمتوسطة علي السطح تزداد في النافورات المعددة (في جميع الترتيبات) عن النافورة الواحدة. وأن معامل انتقال الحرارة يتناسب طرديا مع رقم رينولدز و عكسيا مع البعد عن مركز النافورة. وفي البحث تم وضع منحنيات وجدول رقمية توضح القيم العديدة للمقارنات في الترتيبات المختلفة و كذلك النسبة المئوية.

Keywords: Heat transfer, Free jets, Impinging of multi jets, Experimental heat transfer

1. Introduction

Liquid jet impingement on a surface for transmission of heat from this surface is an effective controllable high heat flux heat transfer method. The applications of the impingement technique are numerous which include annealing of metals, tempering of glass, cooling of electronic equipment and freezing of tissue in cryosurgery. When a large surface has to be heated or cooled, then it is required to use more than one jet. Therefore extensive research on the multiple jets had to be carried out to determine the effect of multiple jets on the heat transfer between the jets and the surface. Film thickness for different jet arrangements were measured experimentally by Farahat [1]. Koopman et al. [2]

determined the local heat transfer coefficient between a row of impinge circular jets on a plane surface. An experimental work was done by Dyban et al. [3] to determine the local heat transfer from a surface blown by an array of round impinging jets with the spent air exhausted on one side. Slayzak et al. [4] have conducted experimental work. to study the effect of interaction between to planner impinging jets on the local heat transfer coefficient. Aaron et al. [5] studied experimentally the effect of jet-jet dimensionless spacing, low nozzle-plate spacing and spent air exits located between the jet orifices on the magnitude and uniformity of the convective heat transfer coefficients. Seyeden et al. [6] presented results of the numerical simulation of two - dimensional flow field and heat transfer

due to laminar heated multiple slot jets discharging normally on to a converging confined channel. Lee et al. [7] conducted an investigation on jet impingement in order to perform comparative analysis with the micro channel cooling. Arjocu et al. [8] studied the characteristic of the impingement heat transfer of a three by three square array of submerged, elliptic impinging jets. Chattopahyay et al. [9] have investigated numerically the turbulent flow field and heat transfer in an array of slot jets impinging on a moving surface by Large-eddy simulation technique in the range of Reynolds numbers between 500 and 3000. Laminar flow and heat transfer on a moving surface due to a bank of impinging slot jets have been numerically investigated by Chattopadhyay and Saha. [10]. Two types of jet, namely axial and knife-jet with an exit angle of 60° were considered. Rahimi, et al. [11] studied impingement heat transfer in an under-expanded axisymmetric air jet. This study is concerned with the heat transfer that occurs when an under expanded jet impinges onto a heated surface. Roy and Patel [12] have studied jet impingement heat transfer and flow for two rectangular jets impinging upon an inclined surface. Heat transfer predictions with a cubic $k-\varepsilon$ model for axisymmetric turbulent jets impinging onto a flat plate is studied by Merci and Dick [13]. Local heat transfer in turbulent axisymmetric jets, impinging onto a flat plate, is predicted with a cubic $k-\varepsilon$ model. Both the constitutive law for the Reynolds stresses and the transport equation for the dissipation rate ε contribute to improved heat transfer predictions. Recently, Kanokjaruvijit et al. [14] studied eight by eight jet array impinging onto a staggered array of dimples. Their study was carried at fixed Reynolds number, $Re=11500$.

From the previous review, the enhancements of heat transfer due to multiple jets and the interaction between them were not examined. Therefore, this research is devoted to study the effect of interactions between the jets and also comparison between the heat transfer in the case of single jet with that for multi jets in different situations.

2. The experimental setup and measuring technique

The general layout of the apparatus is shown in fig. 1. The experiment is implemented with the suitable instruments to control and measure the different variables affecting the phenomena.

2.1. The cooling water circuit

Water is delivered from the main through a control valve to a water storage tank $1.5 \times 1.0 \times 1.0$ m. The tank is connected with 1.25 kW water pump which delivers water to the tank at 4.5m height from the pump level.

2.2. The hot plate

The hot plate is manufactured from stainless steel sheet 2.5 mm thickness. It is mounted on the top of the heating chamber. Each edge of the hot plate is provided with 8 right angle cross bars.

2.3. Heating chamber

It is manufactured from stainless steel sheet. The heating chamber is $90 \times 90 \times 15$ cm and 2 mm wall thickness. The chamber is thermally insulated.

2.4. Steam generator

A steam generator with an electric heater of 18 kW capacity is used to generate the required heating steam. The heater is composed of three-heater elements 6 kW capacity each at 220 V supply. The amount of generated steam is regulated by changing the interconnection between the heaters, the capacity of the heater can be 2 kW, 6 kW, 9 kW, 12 kW or 18 kW. The boiler is insulated with two layers of insulation, the first one is asbestos with 1.27 cm thickness, the other one is glass wool with 3.84 cm thickness.

2.5. Measuring the water film thickness

A micrometer with 0.01 mm sensitivity is used to measure the water film thickness. The micrometer is carried on a specially designed

mechanism, which can be clamped around any one of the PVC tubes. To determine the film thickness, the oscillatory height of the film is first measured and later on an average height can be computed, therefore a special electric circuit similar to that described in reference [15] is used. A D/C power supply manufactured by TRID and capable of producing maximum of 3 Amperes at 25 Volt is made to exert 5 Volt on a 5 k Ω resistance as shown in fig. 2. When the stylus tip is in the air above the liquid film, the oscilloscope is

supposed to read the voltage of the D/C power supply.

2.6. Measuring the temperature

A thermocouple with a protective cover of ceramic fixed on micrometer head as shown in fig. 3 was to used measure temperature gradient through water film and also to measure the temperature of cooling water exit from nozzle, this thermocouple can be

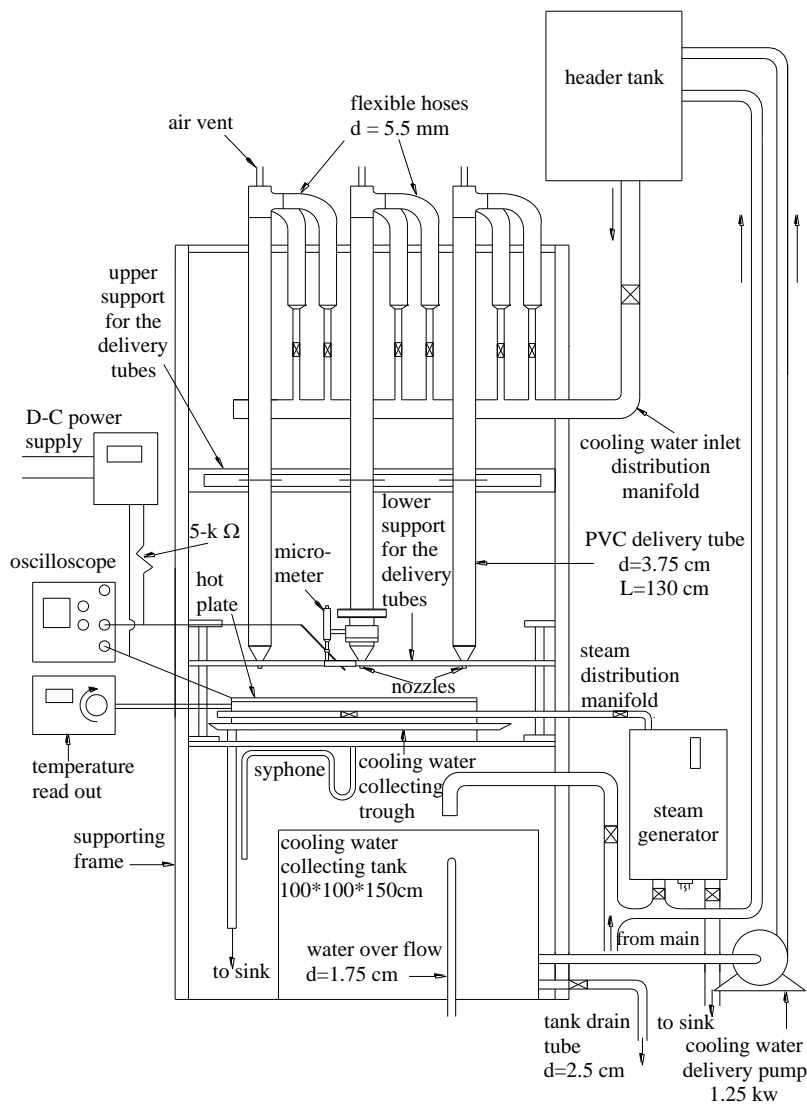


Fig. 1. General layout of the apparatus.

reconnected to the circuit that was used for measuring fluid film thickness. To minimize the thermocouples used for measuring the surface temperature of hot plate, symmetry was considered in thermocouples fixation. Thermocouples are fixed at 79 points as shown in fig. 4. These thermocouples were distributed as follows: 26 thermocouples on line OE, starting from point (O), the center of hot plate, 22 thermocouples on line BF, starting from point (B) and 31 thermocouples on line OG, starting from point (O) at pitches equal 20mm. This distribution was capable to measure the hot plate surface temperature for all situations studied in this research.

3. Data reduction

3.1. Experimental program double jets

This is the simplest case of multiple jets arrangement; fig. 5 shows the jets arrangement for different case study. In the case of double jets, the operating jets are (a)

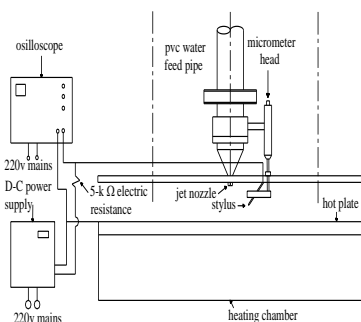


Fig. 2. Oscilloscope circuit for recording the wavy film thickness.

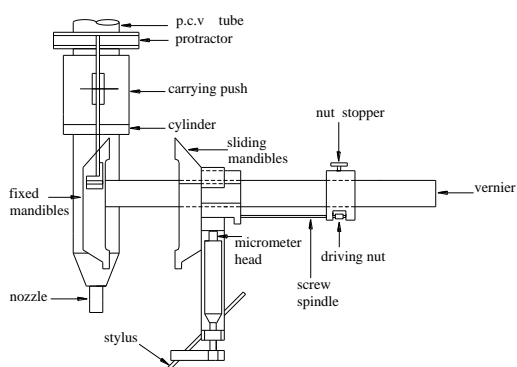


Fig. 3. Mechanism for measuring water film thickness.

and (b), (the jet(a) is located at hot plate center). Film thickness and temperature distribution measurements are carried out around jet (b) and using symmetry, these measuring values around jet (a) can be determined.

The In-line arrangement for three jets: Three jets are distributed on straight line. Measurements of temperature and film thickness are carried out around jet (b) in two cases. In the first case, jets (a), (b) and (c) are only in operation. While in the second case, jets (e), (b) and (d) are only in operation as shown in fig. 5. Jet (b) is considered as a terminal jet in the first case while it is considered as central jet in the second case.

L- Shaped or corner arrangement for three jets: Three jets are distributed in form of L-shape or in form of right angle, as seen in fig. 5. Measurements of film thickness and temperature distribution are carried out around jet (d) in two cases. In the first case, jets (a), (b) and (d), are only in operation. And in the second case, jets (b), (d) and (f) are only in operation. Jet (d) is considered as a terminal jet in the first case while it is considered as a corner jet in the second case. The purpose of studying the above three arrangements is to explore the possibility of predicting the characteristics of the complex cases by the superposition of the characteristics of a number of the above simple situations.

This arrangement is supposed to represent the minimum constructional unit jet array. The minimum unit consists of a three by three

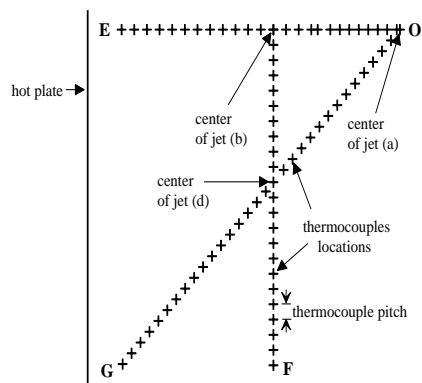


Fig. 4. Locations of thermocouples full cluster arrangement.

array. The longitudinal and transverse pitches are equal. Film thickness and temperature measurements were performed around the jets (a, b and d) only. In all the above arrangements the centerline distances between the jets or the pitches were selected equals to 200 mm. For a nozzle inside diameter of 5.5 mm, this makes the ratio between the jet centerline distance and the nozzle diameter approximately equals to 37. The liquid flow rate through the individual nozzles was varied from 1 to 8 liter/min/jet. From the inspection of the heat transfer of previous results [1] for single jet and the hydrodynamics of multiple jets, it can be seen that the largest values of the Nusselt number of the heat transfer between the liquid and the plate occur near the stagnation point and within the jump area. Also, due to the interaction between the neighboring jets, it is expected that the jump radii between the jets will be smaller than those encountered with a single jet. Therefore, the dimensionless centerline distance or the pitch between the jets was decided to have the value thirty-six. The maximum flow rate value investigated is eight liter per minute, which provides stable laminar flow in the film over the plate. While the minimum value is the one which produces continuous homogenous outflow from the nozzle. The height of the jet nozzle above the plate was kept constant at 40 mm in all experiments. In order to understand the hydraulic interaction between the different jets in all the cases described above, it is necessary to find the effect of this interaction on the local and average Nusselt numbers. In the present work this information will be obtained by direct experimental measurements of the temperature of wall at different locations and the temperature of water film at different positions. Liquid film temperature measurement was executed for the jets a, b, d and f as outlined in fig. 5.

3.1. Heat transfer coefficient

In order to determine heat transfer coefficient, a heat balance was performed on the mass flowing over the plate. From the data taken from the previous results [1] it is

observed that in case of multi jets for any arrangement the fluid film thickness around any jet center line is symmetrical in the shooting flow region but not symmetrical in the streaming flow region, except for central jet in full cluster arrangement which is symmetrical in both regions. The symmetry for measuring the surface temperature for hot plate was used to find the values of temperature at unread points. The coordinates and temperature of the surface points were fed to a computer program "Surfer version 7" to draw isothermal contours representing isothermal wall temperatures, the isothermal contours have oval shapes, sample from these contours is shown in fig. 6. So the area of the plate around jet center is divided into noncircular segments. Each one can be considered at constant temperature with numerical value equals to the arithmetic mean values of the two contours bounded the segment. The area of the segment was measured by a plan meter.

3.1.1. Segment heat transfer coefficient

In order to calculate the segment heat transfer coefficient a heat balance for the flowing water is carried out as follows. The thermal energy absorbed by the flowing water over any segment must be equal to the heat transferred from that segment of the plate to the water film, therefore:

$$\begin{aligned} m(Cp_n \times T_n - Cp_{n-1} \times T_{n-1}) &= A_n \times h_n (T_{un} - T_{n-1}) \\ \therefore h_n &= \frac{m(Cp_n \times T_n - Cp_{n-1} \times T_{n-1})}{A_n (T_{un} - T_{n-1})} \end{aligned} \quad (1)$$

3.1.2. Average segment heat transfer coefficient

A heat balance for the flowing liquid is invoked to calculate the average segment heat transfer coefficient using the principle, thermal energy absorbed by the film must equal to the heat transferred from the hot plate to the film.

$$\bar{h} = \frac{m(Cp_{ex} T_{ex} - Cp_o T_o)}{\sum_1^n A_n (T_{un} - T_o)} \quad (2)$$

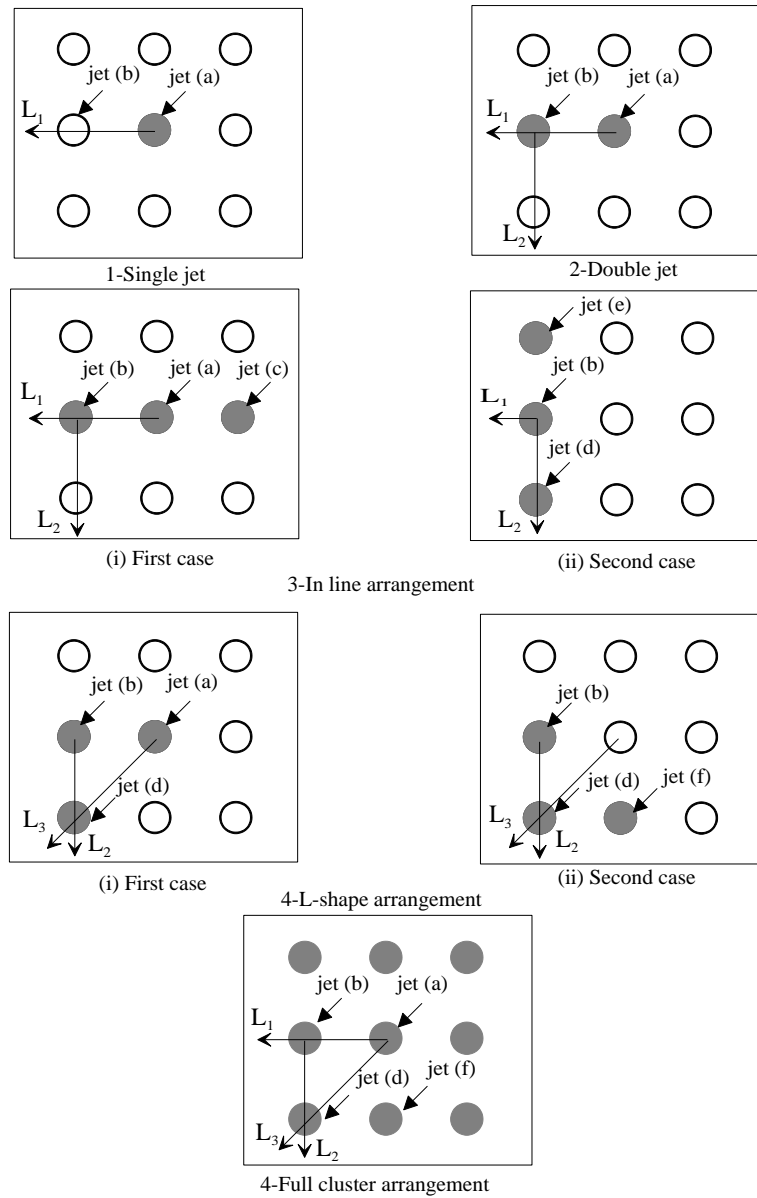


Fig. 5. Jets arrangement.

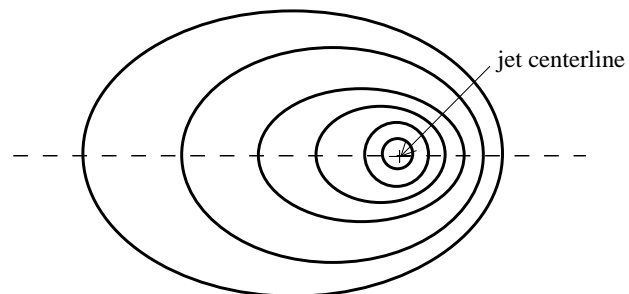


Fig. 6. Isothermal contours and segments.

3.2. Nusselt number

3.2.1. Segment Nusselt number

The segment Nusselt number of plate can be calculated based on segment heat transfer coefficient h_n .

$$Nu_n = h_n d / k . \quad (3)$$

3.2.2. Average segment Nusselt number

The average segment Nusselt number of certain area of the plate can be calculated based on average segment heat transfer coefficient \bar{h}

$$\bar{Nu} = \bar{h} d / K . \quad (4)$$

4. Results, discussions and comparison

This section contains a presentation of experimental results for multi jets arrangements for flow rates of 1, 5 and 8 l/min with a comparison with results for single jet reported by Farahat [15] to show the effect of jets interaction. The segment and average segment Nusselt numbers are presented with respect to dimensionless radius for three selected values of Reynolds number of 5000, 25000 and 40000.

4.1. Double jets

In this case the two jets seem to be approximately identical, so the fluid film thickness, wall temperature and local fluid temperature should be symmetrical on both sides of the line joining the centers of the two jets, therefore the results are presented only for one jet.

4.1.1. Effect of interaction on segment and average segment Nusselt numbers

Figs. 7 and 8 show the effect of interaction on the segment and average segment Nusselt number. It is seen from figures that segment and average segment Nusselt number for single jet and double jet in the three directions (a), (b) and (c) are equal in the shooting flow region because the film thickness values are also equal and not affected by the interaction while in streaming flow region the interaction

tends to increase fluid film thickness. This means reduction in fluid film velocity and consequently reduction in segment Nusselt number and changing the hydraulic jump profile from circular profile into non circular radial profile as observed by Farahat [1]. The film thickness is the highest in (b) direction, that having the maximum interaction and is the lowest in (a) direction. This indicates that the mean fluid film velocity is also the lowest in (b) direction and the highest in (a) direction, so the segment Nusselt number is the highest in (a) direction more than the other directions at certain dimensionless radius. Table 1 shows the percentage of reduction in segment and average segment Nusselt number compared with the single jet at directions (a), (b) and (c). From the tables it is shown that the percent of maximum reduction in both segment and average segment Nusselt number are reduced by increasing Reynolds number therefore the effect of interaction reduced by increasing Reynolds number.

4.2. Three in-line jets arrangement

4.2.1. Effect of interaction on segment and average segment Nusselt number

Similar to double jet, the interaction between jets causes asymmetry for the fluid film thickness around jet centerline. So the same technique used for calculating the segment and average segment Nusselt number for double jet is also applied for the left terminal and central jets in the arrangement. Figs. 9 and 10 show the effect of interaction on the segment and average segment Nusselt number. Similar to double jet the segment and average segment Nusselt number are equal in single jet for both directions (a) and (b) through the shooting flow region while the situation differs in the streaming flow at which the film thickness is increased by the effect of jet interaction, so it is found that the value of both segment and average segment Nusselt number in case of single jet is higher than in the (b) direction and lowest between jets where the interaction reaches maximum. Table 2 shows the reduction percentage in segment and average segment Nusselt number due to interaction compared with the single jet, it is shown that the percent of maximum

reductions in both segment and average segment Nusselt number are reduced by increasing Reynolds number.

4.3. L-shaped arrangement

4.3.1. Effect of interaction on segment and average segment Nusselt numbers

Due to interaction carried out between jets, the film thickness distribution is not symmetrical around jet centerline. Therefore, the same technique used for calculating

segment and average segment Nusselt numbers for double jet is now used. Figs. 11 and 12 show the effect of interaction on the segment and average segment Nusselt number. Similar to double and in line three jets arrangements. The numerical values of both segment and average segment Nusselt numbers are equal to the values for single jet in both directions (a) and (b) through the shooting flow region. On the other hand, in the streaming flow the film thickness is increased by the effect of jet interaction, the

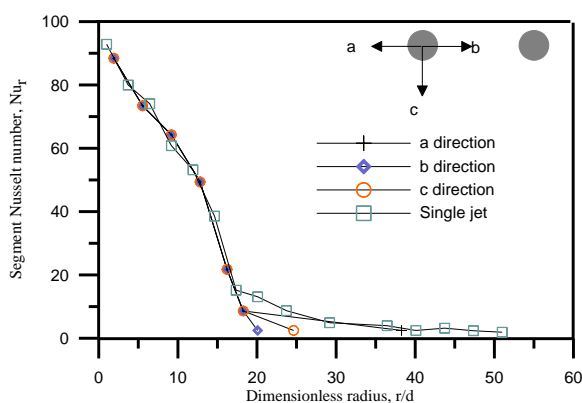


Fig. 7. Segment Nusselt number for double jet $Re =40000$.

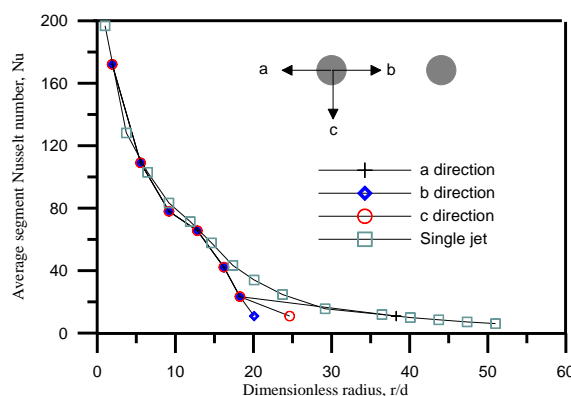


Fig. 8. Average segment Nusselt number for double jet $Re =40000$.

Table 1

Percentage of maximum reduction in segment and average segment Nusselt number of double jets compared with single jet

Re	Percentage of maximum reduction in segment Nusselt number			Percentage of maximum reduction in average segment Nusselt number		
	(a) direction	(b) direction	(c) direction	(a) direction	(b) direction	(c) direction
5000	18.5%	69.7%	65.3%	32.6%	68%	61%
25000	17.5%	64%	40%	18.2%	62%	40%
40000	15%	56.2%	26%	17.3%	56.2%	25.3%

Table 2

Percentage of maximum reduction in segment and average segment Nusselt number for three in line jets compared with single jet

Re	Percentage of maximum reduction in segment Nusselt number		Percentage of maximum reduction in average segment Nusselt number	
	(a) direction	(b) direction	(a) direction	(b) direction
5000	70.2%	68%	69.4%	60.3%
25000	66.1%	49.9%	63.9%	51.2%
40000	62.4%	35%	56.7%	36%

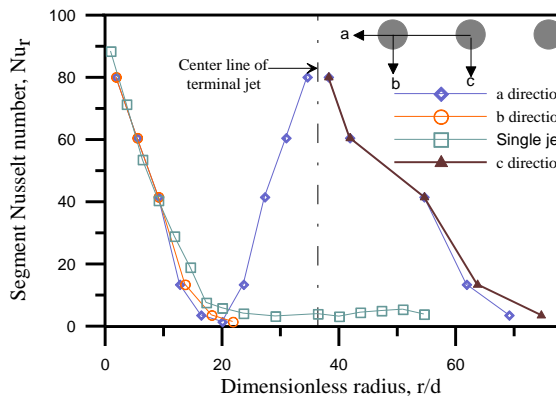


Fig. 9. Average segment Nusselt number for 3-jets in line arrangement $Re=40000$.

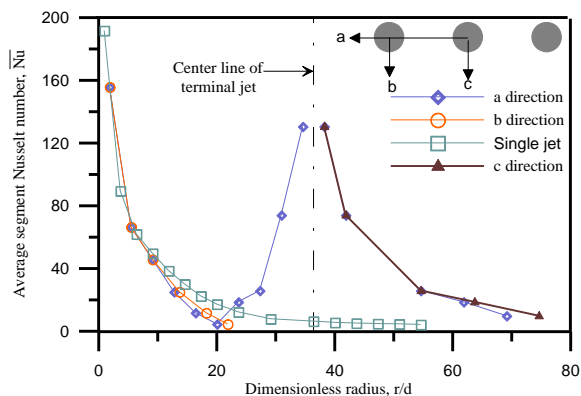


Fig.10. Average segment Nusselt number for 3-jets in line arrangement $Re=25000$.

segment and average segment Nusselt number is higher in single jet, lower in (b) direction and lowest between the corner and terminal jets. This means that, the interaction reaches maximum value at this region. Table 3 shows the percentage of reduction in segment and average segment Nusselt number compared with that in the single jet indicating the effect of interaction on heat transfer. It is shown that the percent of maximum reduction in both segment and average segment Nusselt number for L-shaped arrangements are reduced by increasing Reynolds number as in the previous cases of double jet and in three in-line jet arrangements. The average segment Nusselt number for single jet and corner jet are equal in shooting flow region while it is lower in case of central jet in the streaming flow region.

4.4. Full cluster arrangement

4.4.1. Effect of interaction on segment and average segment Nusselt numbers for central jet

For all Reynolds numbers, it is observed from data taken from previous work [1] that for central jet the fluid film thickness is symmetrical about its center line, therefore it is treated as single jet to determine the segment and average segment Nusselt numbers. Figs. 13 and 14 show a comparison between results of single jet [15] and central

jet of full cluster to illustrate the effect of interaction on segment and average segment Nusselt numbers for the central jet. The interaction tends to reduce the hydraulic jump radius and increase fluid film thickness in the streaming flow region only. Therefore the segment and average segment Nusselt number for single jet and central jet are equal in shooting flow region, while they are lower for central jet in the streaming flow region. table 4 illustrates the maximum reduction percent of both segment and average segment Nusselt numbers for central jet compared with single jet. Similar to the previous arrangements, it is shown from table 4 that the percent of maximum reduction in both segment and average segment Nusselt numbers are reduced by increasing Reynolds number.

4.4.2. Effect of interaction on segment and average segment Nusselt numbers for left terminal jet in the middle row and for corner jet in the left of lower row

For the left terminal jet in the middle row the fluid film thickness about its center line is not symmetrical, therefore it is treated with the same procedures as in case of double jet to determine the segment and average segment Nusselt numbers. According to the data taken from the previous work [1], it is observed that the fluid film thickness distribution on both sides of line joining the centers of left terminal jet and central jet on

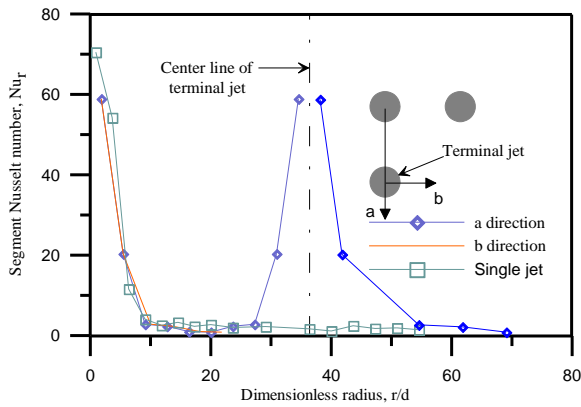


Fig. 11. Segment Nusselt number for L-shape arrangement $Re=5000$.

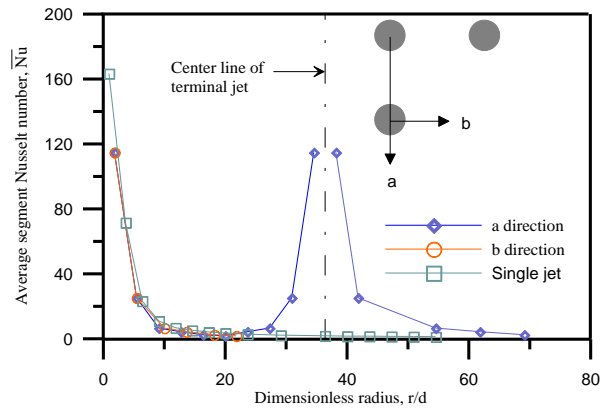


Fig. 12. Average segment Nusselt number for L-shape arrangement $Re=5000$.

Table 3

Percentage of maximum reduction in segment Nusselt number for L- shaped compared with single jet

Re	Percentage of maximum reduction in segment Nusselt number		Percentage of maximum reduction in average segment Nusselt number	
	(a) direction	(b) direction	(a) direction	(b) direction
5000	80.2%	78%	84.7%	81.5%
25000	70%	59%	72%	60.5%
40000	66.5%	39.8%	60%	39.9%

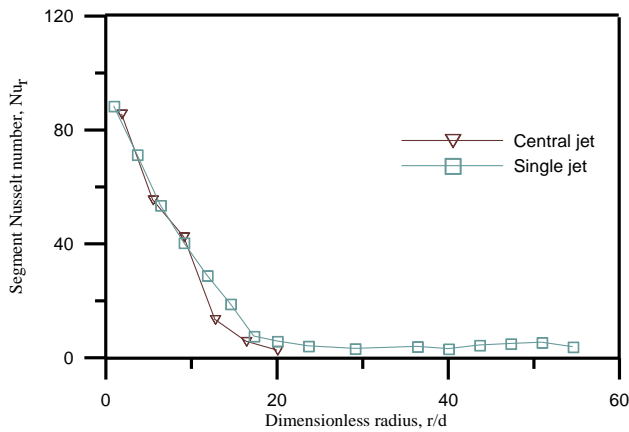


Fig. 13. Segment Nusselt number for central jet of full cluster for $Re=25000$.

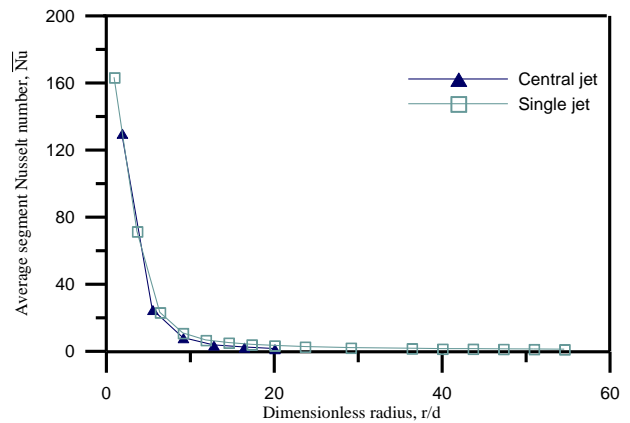


Fig. 14. Average segment Nusselt number for central jet of full cluster for $Re=5000$.

Table 4

Percentage of maximum reduction in segment and average segment Nusselt number for central jet of full cluster arrangement compared with single jet

Re	Percentage of maximum reduction in segment Nusselt number	Percentage of maximum reduction in average segment Nusselt number
5000	84.4%	87.3%
25000	74.5%	76.4%
40000	69.4%	62%

the middle row is symmetrical, so it is expected that both segment and average segment Nusselt numbers are also symmetrical. For corner jet in the left of lower row, the fluid film thickness is not symmetrical about its centerline while it is symmetrical on both sides of line joining its centerline with centerline of central jet. Figs. 15 and 16 show a comparison for the segment

and average segment Nusselt number between the left terminal jet in the middle row of the present arrangement and single jet for flow rate of 5 l/min. It is observed that both segment and average segment Nusselt number are approximately the same in single jet and in (a, b and c) directions in shooting flow region. It is also seen that both segment and average segment Nusselt number in (b and c)

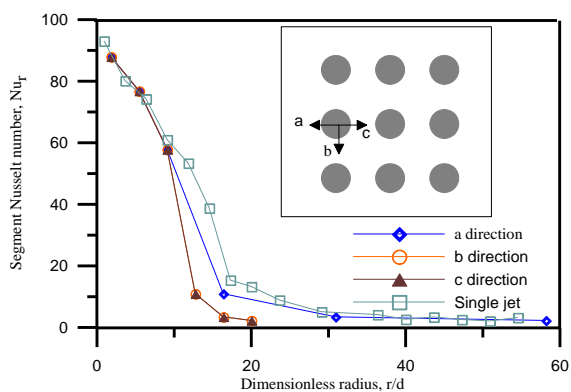


Fig. 15. Segment Nusselt number for terminal jet of full cluster Re=40000.

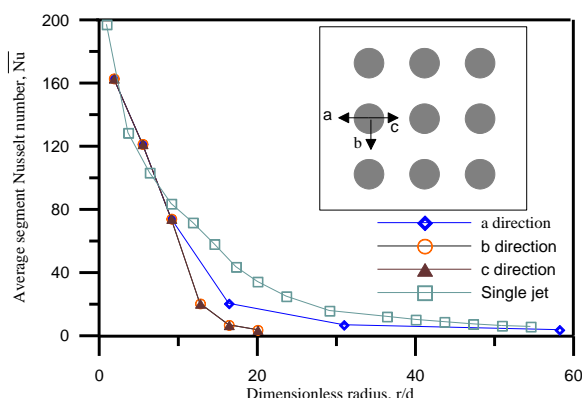


Fig. 16. Average segment Nusselt number for terminal jet of full cluster Re=40000.

Table 5

Percentage of maximum reduction in segment and average segment Nusselt number for the left terminal jet in the middle row compared with the single jet

Re	Percentage of maximum reduction in segment Nusselt number			Percentage of maximum reduction in average segment Nusselt number		
	(a) direction	(b) direction	(c) direction	(a) direction	(b) direction	(c) direction
5000	24%	84.4%	24%	37.6%	87.3%	37.6%
25000	20%	74.5%	20%	21%	76.4%	21%
40000	17%	69.4%	17%	19%	62%	19%

Table 6

Comparison between single and multi jets

Arrangement	Reynolds number per one jet	Average Nusselt number	Improving percent in average Nusselt number compared with single jet
Double jet	5000	24.13	21%
	25000	71.88	80%
	40000	83.32	86%
3-in line	5000	30.3	52%
	25000	81.94	106%
L-shaped	40000	114.27	155%
	5000	27.1	36%
Full cluster	25000	76	91%
	40000	104.7	134%
	5000	69.11	247%
	25000	145.8	266%
	40000	200.35	348%

directions are equal, because the fluid has the same film thickness in both directions and they are lower than in (a) direction in the streaming flow region for the same reason as in double jet. Table 5 shows the percentage of reduction in segment and average segment Nusselt numbers compared with the single jet transfer. From the table it is shown that the percent of maximum reduction in both segment and average segment Nusselt numbers are reduced by increasing Reynolds number.

4.5. Comparison between single and multi jets

As explained in the previous sections, the interaction between jets tends to reduce both segment and average segment Nusselt number for one jet of the multi jets compared with single jet but the overall average Nusselt number for multi jets for any arrangement is higher than single jet with flow rate equals to that of one jet of the multi jets. This can be illustrated from table 6. For any arrangement in multi jets in table 6 the average Nusselt number is calculated per jet, and taking the algebraic summation to get the overall average Nusselt number for the arrangement. All Reynolds numbers given in that table is per one jet. It is clear that the improving in average Nusselt number is increased with increasing number of jets therefore multi jets are better than single jet for the rate of heat transfer and full cluster arrangement has the highest average Nusselt number. So the total heat transfer is enhanced by increasing the number of jets. It is observed that the thermal performance for three jets in in-line arrangement is better than that for three jets in L-shaped arrangement, therefore if only three jets are available for cooling a hot plate, so it is better to arrange them in-line form.

5. Conclusions

An interaction is observed between the jets which leads to reduce the mean velocity of the fluid film which appears in increasing the film thickness specially in the area between the jets, this in turn tends to reduce both segment and average segment Nusselt numbers. The effect of interaction is higher in the area between jets and is minimum at the free end

of the jet. The effect of interaction between jets in multi jets tends to reduce both segment and average segment Nusselt numbers for one jet of the multi jets compared with single jet but the overall average Nusselt number for multi jets for any arrangement is higher than single jet with flow rate equals to that of one jet of the multi jets. It is observed that, the interaction is decreased at higher Reynolds number and the improvement in average Nusselt number is increased with increasing number of jets. Therefore multi jets are better than single jet for rate of heat transfer and full cluster arrangement has the highest average Nusselt number. For engineering applications, in order to enhance the heat transfer it is required to increase number of jets. To reduce the effect of the interaction between the jets, it is necessary to increase nozzle-to-nozzle spacing or to increase the fluid flow rate. More over the thermal performance for three jets in line arrangement is better than that for three jets in L-shaped arrangement. Therefore if only three jets are available for cooling a hot plate it is better to arrange them in line form.

Nomenclature

A_n	is the area of segment n, m^2 ,
C_p	is the specific heat, $J/kg K$,
d	is the nozzle diameter, m ,
g	is the gravity acceleration, m/s^2 ,
H	is the nozzle to plate separating distance, m ,
h	is the average segmental heat transfer coefficient, $W/m^2 K$,
h_r	is the segmental heat transfer coefficient, $W/m^2 K$,
K	Is the fluid thermal conductivity, $W/m K$,
Nu_r	is the segment Nusselt number, $h_r d/K$,
Q	is the water volume flow rate, m^3/s ,
q	is the heat flux, W/m^2 ,
r	is the radial coordinate, m ,
Re	is the reynolds number, $V_j d/\nu$,
T	is the fluid temperature, $^{\circ}C$,
T_o	is the jet temperature, $^{\circ}C$,
T_w	is the wall temperature, $^{\circ}C$,
V_j	is the jet velocity, m/s ,
Z	is the axial coordinate, m ,
Z'	is the dimensionless axial component, z/d , and

Z is the average water film thickness, mm.

Greek symbols

α is the thermal diffusivity, m^2/s ,
 μ is the dynamic fluid viscosity, $kg/m\ s$,
 ν is the kinematics fluid viscosity, m^2/s .
 ϕ is the angular coordinate, rad,
 ρ is the fluid density, kg / m^3 ,
 θ is the dimensionless temperature,
 $(T-T_0)/(T_w-T_0)$, and
 σ is the coefficient of surface tension, N/m .

References

- [1] S. Farahat, "Fluid Flow and Heat Transfer Due to Multi Jets Normal to Flat Plate," M. Sc. Thesis, Dep. of Mechanical Engineering, Univ. of Alexandria, January (1996).
- [2] R.V. Koopman and E.M. Sparrow, "Local and Average Transfer Coefficients Due to an Impinging Row of Jets "Int. J. Heat Mass Transfer, Vol. 19, pp. 674-683 (1975).
- [3] E.P. Dyban, A.I. Mazur and V.P. Golavanov, "Heat Transfer and Hydrodynamics of an Array of Round Impinging Jets With One-Sided Exhaust of the Sprint Air " Int. J. Heat Mass Transfer, Vol. 23, pp. 667-676 (1979).
- [4] S.J. Slyzak, R. Viskanta and F.P. Incropera, "Effects of Interaction Between Adjacent Free Surface Planner Jets on Local Heat Transfer From the Impingement Surface," Int. J. Heat Mass Transfer, Vol. 37, pp. 269-282 (1993).
- [5] A. M. Hubor and R. Viskanta, "Effect of Jet-Jet Spacing, Convective Heat Transfer to Confined, Impinging Arrays of Axisymmetric Air Jets" Int. J. Heat Mass Transfer, Vol. 37, pp. 2859-2869 (1994).
- [6] S.H. Seyedein, M. Hasan and A.S. Mujumdar, "Laminar Flow and Heat Transfer From Multiple Impinging Slot Jets With an Inclined Confinement surface," Int. J. Heat Mass Transfer, Vol. 37, pp. 1867-1875 (1993).
- [7] D.Y. Lee, K. Vafai, "Comparative Analysis of Jet Impingement and Microchannel Cooling For High Heat Flux Applications" Int. J. Heat Mass Transfer, Vol. 42, pp. 1555-1568 (1998).
- [8] S.C. Arjou and J.A. Liburdy, "Identification of Dominate Heat transfer Modes Associated With The Impingement of an Elliptical Jet Array" ASME Journal of Heat Transfer, Vol. 122, pp. 240-247 (2000).
- [9] H. Chatlopadhyay, G. Biswas and N.K. Mitra, "Heat Transfer From a Moving Surface Due to Impinging Slot Jets" ASME Journal of Heat transfer, Vol. 124, pp. 433-440 (2002).
- [10] H. Chattopadhyay and S.K. Saha, "Simulation of Laminar Slot Jets Impinging on a Moving Surface" ASME Journal of Heat transfer, Vol. 124, pp. 1049-1055 (2002).
- [11] M. Rahimi, I. Owen and J. Mistry, "Impingement Heat Transfer in an Under-Expanded Axisymmetric Air Jet," Int. J. Heat Mass Transfer, Vol. pp. 263-272 (2003).
- [12] S. Roy and P. Patel, "Study of Heat Transfer for a Pair of Rectangular Jets Impinging on an Inclined Surface," Int. J. Heat Mass Transfer, Vol. 46, pp. 411-425 (2003).
- [13] B. Merci and E. Dick, "Heat Transfer Predictions With a Cubic $K-\epsilon$ Model for Axisymmetric Turbulent Jets Impinging onto a Flat Plate," Int. J. Heat Mass Transfer, Vol. 46, pp. 469-480 (2003).
- [14] K. Kanokjaruvijit and R.F. Martinebotas "Jet Impingement on a Dimpled Surface With Crossflow Schemes," Int. J. of Heat and Mass Transfer Vol. 48, pp. 161-170 (2005).
- [15] S. Farahat, "Heat Transfer And Flow Due To Impinging Circular Jets On A Heated Horizontal Surface," Ph D. Thesis, Dep. of Mechanical Engineering, Univ. of Alexandria, May (2003).
- [16] Y.A. Cengel, "Heat Transfer" McGraw-Hill, New York (1999).

Received March 10, 2004

Accepted July 9, 2004